Cosmological Constraints with Strong Gravitational Lensing

Jamie C. McCullough
Department of Physics
Kavli Institute of Particle Astrophysics and Cosmology
Stanford University
jmccull@stanford.edu

June 28, 2023

Abstract

In the era of precision cosmology, models are most compelling when constrained by many different measurement techniques. One promising method that will only improve in precision over the next few years is use of gravitational lensing - as it is sensitive to all types of matter indiscriminately. While strong lensing time delay measurements using variable sources like supernovae and quasars can constrain h, Ω_m, Ω_Λ, this paper will also discuss constraints from weak lensing on Ω_m and σ_8. Underlying physics in a strong lensing system is explained at an introductory level and the state of the literature and future observing implications are discussed.

Keywords Gravitational Lensing · Cosmology · Strong Lensing

Contents

1 Introduction

Measuring cosmic distances and observing the kinematics and geometry of the universe is crucial to our understanding of the evolution of our universe. Much of cosmology has to do with finding an accurate meterstick to lay across the cosmos and checking these measurements against theories that claim to govern them. Both Hubble's discovery of the expansion of the universe and the discovery of the *acceleration* of that expansion rely heavily on standard candles for these distance measurements. There are many techniques to attack the distance problem, but this paper will focus on using gravitational lensing to do so, with a focus on strong lensing time delay measurements [1].

Gravitational lensing is the deflection of light through spacetime by massive bodies as described by General Relativity. While the majority of these cases observed are only small distortions of the source, applying slight shears known as *weak lensing*, in the presence of very strong lenses with opportunely placed sources behind them we may see highly warped, magnified, and even duplicated images originating from behind the lensing structure. With variable sources and multiple light paths of differing lengths, this gives us a means to measure accurate distances by viewing light from a single source take multiple paths to the observer. This has the advantage of being completely independent of standard candle measurements or the cosmological distance ladder. It also will require a good understanding of the mass that deflects the light, which has the potential to be a large systematic uncertainty if not well constrained.

Motivating the need for lensing experiments, all lensing techniques provide unparalleled mass estimation for systems on different scales: weak lensing in the domain of large scale structure, strong lensing in the domain of halo and subhalo structure or galaxy clustering, and microlensing for detections on planetary or stellar scales. This is a powerful probe for the nature of dark matter that covers more than 16 orders of magnitude in size, and 19 orders of magnitude in mass with modern instrumentation [2]. Strong lensing systems can magnify background sources, and the magnification bias in lensing clusters depends on the curvature of the universe (Ω_κ), and this same magnification can allow us to study spectroscopic detail in fainter and more distant galaxies than our telescopes could reach otherwise. Similarly as I broadly mentioned before, the time delay measurements from variable sources behind a lens helps us constrain the Hubble constant, and to a weaker degree our choice of cosmological parameters, Ω_m and Ω_Λ without requiring standard candle calibration. Weak lensing, on the other hand, provides a much larger scale for the matter distribution, allowing us to measure the density contrast and "clumpiness", σ_8, of matter structure that has evolved from the first fluctuations visible in the cosmic microwave background (CMB). Being able to connect early universe probes to the universe we see today is crucial to testing our physical understanding of cosmology, and the CMB paired with weak lensing in surveys supplies complementary data sets.

In this paper I will first introduce the Friedmann equation of state that governs the ΛCDM model for the expansion of the universe and the various cosmological parameters of interest. Then I will discuss the general lensing geometry before outlining the physics behind using time delay measurements in strongly lensed systems to gain cosmological constraints. Future projections for strong lensing and systematic uncertainties will follow. Finally, some broad discussions of the applications of weak lensing on cosmological parameters will be outlined prior to conclusions.

1.1 The Friedmann Equation of State

Beginning in a with a Friedmann-Lemaitre-Robertson-Walker (FLRW) metric we can derive an equation of state for the stress energy tensor, T, of a perfect fluid, described by an energy density and a pressure with the trace. The derivation follows from elements described in Carroll [3].

$$T^{\mu}{}_{\mu} = -\rho + 3p \tag{1}$$

The zero-component provides us with an equation of state within the Einstein equation, if we assume a simple relationship between the density and pressure independent of time. We take the scale factor to be a, and w to be some constant.

$$p = w\rho \tag{2}$$

$$\rho \propto a^{-3(1+w)} \tag{3}$$

Now we use our perfect fluid stress energy tensor to source gravity in Einstein's equation to obtain the two Friedmann equations, Eq. 5 and 6 from the time and spatial components, R is the Ricci tensor, g is the metric, κ is a curvature parameter with units of inverse-square distance,and G is our gravitational constant. These equations govern the expansion of the universe through the evolution of the scale factor, as determined b relativity for a Friedmann-Robertson-Walker universe.

$$R_{\mu\nu} = 8\pi G(T_{\mu\nu} - \frac{1}{2}g_{\mu\nu}T) \tag{4}$$

$$\left(\frac{\dot{a}}{a}\right)^2 = \frac{8\pi G}{3}\rho - \frac{\kappa}{a^2} \tag{5}$$

$$\frac{\ddot{a}}{a} = -\frac{4\pi G}{3}(\rho + 3p) \tag{6}$$

At last we define the Hubble constant, H_0 and $h = H_0/100$ in terms of the scale factor, as a measure of the expansion of the universe at some given time: $H_0 = \dot{a}/a$.

1.2 The ΛCDM Model of the Universe

We can then define several density parameters, Ω_i that allow us to write the Friedmann equations in terms of the constituent parts of the universe. While matter and radiation have known equations of states, dark energy Ω_Λ is thought to be a cosmological constant. This is generally done in terms of the critical density, $\rho_{crit} = 3H_0^2/8\pi G$, which would be the density for a flat universe. Thus for each dimensionless density parameter we have the following, where we can treat the cosmological constant like a vacuum density. Several of these equations are courtesy of Schneider [4].

$$\Omega_m = \frac{\rho_{m,0}}{\rho_{crit}}; \quad \Omega_r = \frac{\rho_{r,0}}{\rho_{crit}}; \quad \Omega_\Lambda = \frac{\Lambda}{3H_0^2} \tag{7}$$

Additionally, most evidence points to a seemingly flat universe where the curvature is almost negligible, but we can include a curvature term that similarly contributes.

$$\Omega_\kappa = 1 - \Omega_m - \Omega_r - \Omega_\Lambda \tag{8}$$

This allows us to rewrite the Friedmann equations with each component evolving according to the scale factor and their equation of state, in what we call the ΛCDM model of cosmology, or the Λ *Cold Dark Matter* model. *Cold* here refers to the nature of dark matter as slow with respect to the speed of light, meaning that it fits into our assumptions for an analogous perfect fluid with zero pressure.

$$H^2(t) = H_0^2\left[a^{-4}\Omega_r + a^{-3}\Omega_m + a^{-2}\Omega_\kappa + \Omega_\Lambda\right] \tag{9}$$

And finally if we generalize the behavior of Ω_Λ using w, we have could have an additional dependence on the scale factor, which is described by the wCDM model rather than a true cosmological constant. Note that another potential cosmological model allows for time variability in Ω_Λ with a secondary w_a parameter.

$$H^2(t) = H_0^2\left[a^{-4}\Omega_r + a^{-3}\Omega_m + a^{-2}\Omega_\kappa + a^{-3(1+w)}\Omega_\Lambda\right] \tag{10}$$

2 The Theory of Strong Lensing and Time Delays

It is useful to establish the essential geometry to a lensing system, and the approximations acceptable. Firstly, let us define the useful variables and notation.

- D_s, D_d The angular diameter distances to the source and the lens respectively.
- D_{ds} The angular diameter distance between the lens and the source, such that $D_s - D_d = D_{ds}$.
- $\hat{a}$ The deflection angle of the ray passing by the mass in the thin lens approximation.
- ξ The separation from the light ray from the optical axis through the lens as a two dimensional vector in the lens plane.

We can see the basic geometry for a lensed system supplied in Fig. 1(a). The derivation of the general lens equation was drawn primarily from Schneider's text *Gravitaional Lenses* [5]. From this geometry, we find that the relation between the unlensed position angle, β, and the true position as seen by the observer, θ, is given by the simple lens equation.

$$\beta = \theta - \frac{D_{ds}}{D_s}\hat{a}(\xi) \tag{11}$$

In a strongly lensed system, when multiple images form from the same source the light seen can take multiple paths and still reach the observer. If the source has temporal variation in flux, for example a quasar or supernova, the delay between observed events in each image depends very precisely on the distances measured and the properties of the lensing system. In fact, it is easy to see how the difference in arrival time, Δt would be highly sensitive to the Hubble constant as it is effectively a distance measurement.

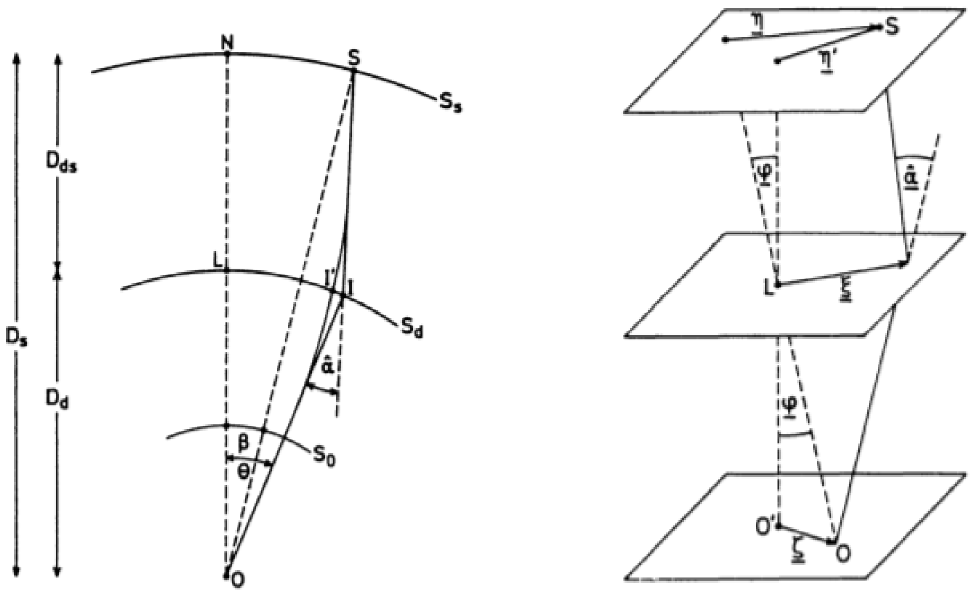

(a) The lensing geometry, depicted here shows the observer, O, viewing light from a source, S, after it is deflected through the lens, L.

(b) Variable definition and general geometry to derive the time delay measurement.

Figure 1: The angular geometry (left) and the three dimensional definition (right) for a lensed system. Figures courtesy of Schneider [5].

The distances measured can come in two forms if combined with a lens mass model and lens stellar kinematics: the time delay distance, and the angular diameter distance. The first, as previously discussed best constrains H_0, while the second can help probe Ω_Λ and w if we have sources at multiple redshifts behind the lens to work with. The latter phenomenon will be not be discussed in depth while the former is discussed here.

The time delay is comprised of two components.

- ***Geometric:*** The time light takes to travel the physical path difference.
- ***Shapiro:*** The general relativistic time dilation from the two rays experiencing different depths of the lens potential.

According to Fermat's principle, known as the *principle of least time*, light takes the path between two points that requires the shortest time.We define a Fermat potential, $\phi(x, y)$ with respect to the gravitational potential, ψ, where we can define the observer position in dimensionless form as $y = \eta/\eta_0$, and the dimensionless $x = \xi/\xi_0$ as the location where the light rays cross the lens plane. This scalar potential is the time delay function of the lens, and holds true because the deflection angle can be written as $\alpha = \nabla\psi$.

$$\phi(x, y) = \frac{1}{2}(x - y)^2 - \psi(x) \tag{12}$$

Recall that the relation between angular diameter distance, D_A, and comoving transverse distance, D_M is redshift dependent and written as

$$D_A = \frac{D_M}{(1 + z)}. \tag{13}$$

We define y as a dimensionless equivalent to the observer position ζ according to the geometry described in Fig. 1(b) in such a way that $\eta' = 0$, which leaves us with a reduced version of the lens equation (Eqn. 11) that will not be derived here for the sake of brevity. The redshift enters the equation via Eqn. 13 to relate the angular distance at the lens in the same space as distance at the observer.

$$y = \frac{1}{\eta_0} \frac{D_{ds}}{D_d(1+z_d)} \zeta. \tag{14}$$

$$d\zeta = (1+z_d)\xi_0 \frac{D_s}{D_{ds}} dy \tag{15}$$

If we have two positions ξ_1, ξ_2, the angular separation between the two, υ, is simple geometry. Recall that x is the dimensionless equivalent of ξ scaled by ξ_0, which is an arbitrary length scale chosen in the lens plane, and we choose the other length scale in the source plane to be $\eta_0 = \xi_0 D_s / D_d$.

$$\upsilon = \frac{\xi_2 - \xi_1}{D_d} = \frac{\xi_0(x_2 - x_1)}{D_d} \tag{16}$$

Using this angular separation and the geometry of the system, the time delay can be recovered by integrating the expression below [5].

$$d(c\Delta t) = \upsilon \cdot d\zeta \tag{17}$$

$$c\Delta t = \int_{\zeta_0}^{\zeta} \upsilon(\zeta') \cdot d\zeta' + c\Delta t(\zeta_0) \tag{18}$$

If we use Eqns. 15 and 16, and evaluate the integral we at last get something we can write in terms of our potential (Eqn. 12).

$$c\Delta t(y) = \xi_0^2 \frac{D_s}{D_d D_{ds}} (1+z_d) \left[\phi(x_1, y) - \phi(x_2, y)\right] \tag{19}$$

Looking at Eq. 19, we see that our choice of ϕ from the lens equation is a good one, as this equation indicates that ϕ is proportional to the light travel time only with geometric prefactors.

$$T(x,y) = \frac{\xi_0^2}{c} \frac{D_s}{D_d D_{ds}} (1+z_d) \left[\phi(x,y)\right] \tag{20}$$

This is true, and the Fermat potential can be written in terms of the gravitation deflection potential at $\psi(x)$ and positions so that we find the travel time to be

$$T(x,y) = \frac{\xi_0^2}{c} \frac{D_s}{D_d D_{ds}} (1+z_d) \left[\frac{(x-y)^2}{2} - \psi(x)\right] \tag{21}$$

And we simplify to our final form by simply choosing our length scale precipitously such that $\xi = D_d$, since it makes our nondimensional positions into angular positions as seen by the observer, where $x_i = \theta_i$ for each image and $y = \beta$ is the true position.

$$\Delta t(\beta) = \frac{1}{c} \frac{D_d D_s}{D_{ds}} (1+z_d) \left[\phi(\theta_1, \beta) - \phi(\theta_2, \beta)\right] \tag{22}$$

So for a given mass model, with lens behavior well constrained, we can approximate ϕ and therefore the expected Δt given an assumed cosmology. Since we measure Δt, the angular diameter distance prefactor in Eqn. 22 is approximately inversely proportional to H_0, it is sometimes written as $D_{\Delta t}$[1]. When there are many lenses along the line of sight, this type of distance related prefactor becomes more complex, but the dependence on cosmology remains intact [6].

3 Cosmological Constraints Past and Future: H_0, w, Ω_m

Looking at real Hubble constant inference with 18 strong lenses done by Paraficz & Hjorth 2010, typically an approximate cosmology is assumed (flat, $\Omega_\Lambda = 0.7, \Omega_m = 0.3$) and mass maps are derived for each lens. Even with such a sparse sampling, 1σ constraints on H_0 were measured to be $66^{+6}{}_{-4}$ km/s/Mpc [7]. This already approaches the level of other cosmological probes while not even coming close to saturating the data set.

As more large scale surveys come online in future years, and lensing-specific observing strategies are implemented the numbers of well sampled, Strongly Lensed Time Delay (SLTD) observations will rise and allow the aggregation of data sets to become competitive with other cosmological probes. Fig. 2(b) depicts how multiple STLD systems is forecasted to affect the precision of the inferred wCDM parameters with simulated lensing systems. Here, with a ΛCDM model and 1000 measured lenses (not an unrealistic estimate for LSST), H_0 could be constrained as well

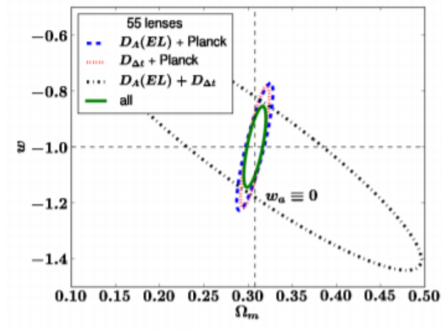

(a) When combined with Planck data (CMB), we see that degeneracy is broken in the $\Omega_m - w$ plane with time delay measurements and lens distance measurements [9].

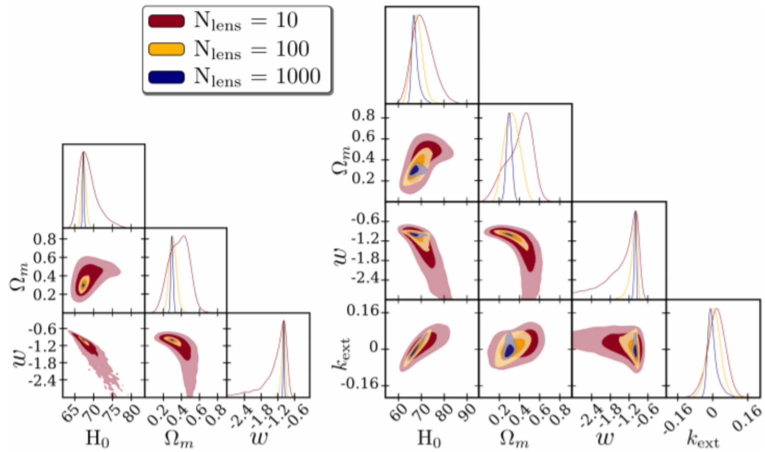

(b) The addition of more strong lensing systems will significantly better the precision of constraints on wCDM parameters in Shiralilou et al. [8].

Figure 2: The forecast (right) for the additional lenses and the degeneracy breaking (left) using angular diameter distance and time delay distance with Planck.

as 0.1%, whereas a varying equation of state for dark energy raises the error up to 1% for the same number of lenses [8]. This conclusion was drawn by generating lens potentials in a fiducial cosmology and mocking lenses uniformly distributed across $0 < z \leq 1$ with softened power law elliptical potentials. As with much of cosmology, the posterior was sampled using Monte-Carlo Markov-Chains (MCMC) after formulating the appropriate likelihood. That is to say, the cosmology appropriate for a set of measurements can be found with a standard Bayesian approach, and strong degeneracies between parameters can cause convergence to the *true* cosmology to be difficult.

Specifically, time delay distances ($D_{\Delta t}$) allow the measurement of H_0, but also can break degeneracies in models for the evolution of Ω_Λ when the angular distance (D_L) is constrained by stellar velocity dispersion as can be seen in Fig. 2(a), where the Planck constraint is significantly improved when combined with a sample of 55 well measured lenses [9]. Orthogonally degenerate probes in parameter space are ideal and made possible when probes incorporate independent physical quantities.

In fact, when compared with other cosmological probes, strong lensing is competitive when just 100 systems are well measured (sub 5% $D_{\Delta t}$ precision) according to a forecast by Coe et al. 2009 [10]. This sample forecast is shown in Fig. 3, where it is comparable with Baryon Acoustic Oscillations (BAO) when dealing with H_0 and w_0 measurements. Given that future observations will far exceed this desired precision and sample size, strong lensing will rapidly begin to match the state-of-the-art. Coe predicts that LSST time delay measurements will constrain the Hubble constant to within 0.7%, Ω_Λ to 0.5%, and w to 2.6% (at 1σ precisions) [10]. Also visible in this plot is the way degeneracies intersect, with supernovae and time delay lensing supplying an almost orthogonal set in the $H_0 - w_0$ plane, and BAO supplying degeneracy breaking in the $H_0 - \Omega_k$ plane. This is a conservative look, as sub 5% precision on time delay distances is feasible with modern instrumentation.

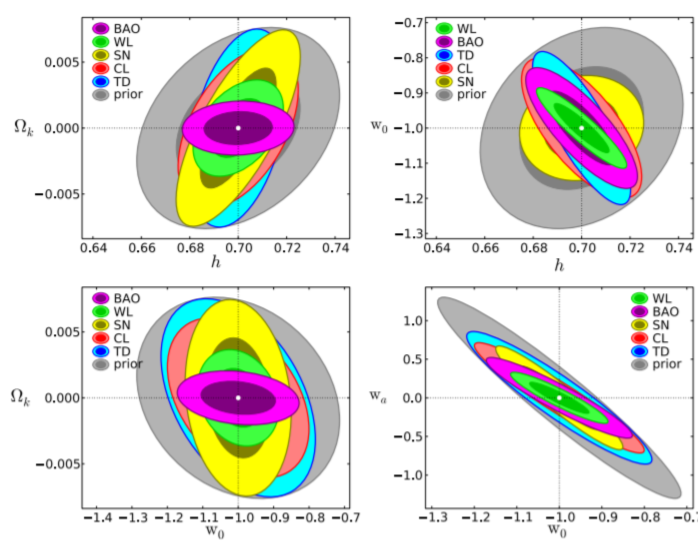

Figure 3: A comparison of next stage constraints on time delays (TD), weak lensing (WL), supernovae (SNe), baryon acoustic oscillations (BAOs) and cluster counts (CLs) in a cosmology with curvature and time variable w_a from Coe 2009 [10].

Similarly, ensemble predictions for future precision on time delay distance measurements are outlined in Fig. 4, with both conservative and favorable estimates that indicate ensemble precision in $D_{\Delta t}$ will improve from the 2-3% level today to below 0.8% with the advent of the Large Synoptic Survey Telescope (LSST) [1]. This precision must be on the ensemble level, because systematics governing individual lens systems (external convergence, for example) will dominate if not handled accordingly and uniformly.

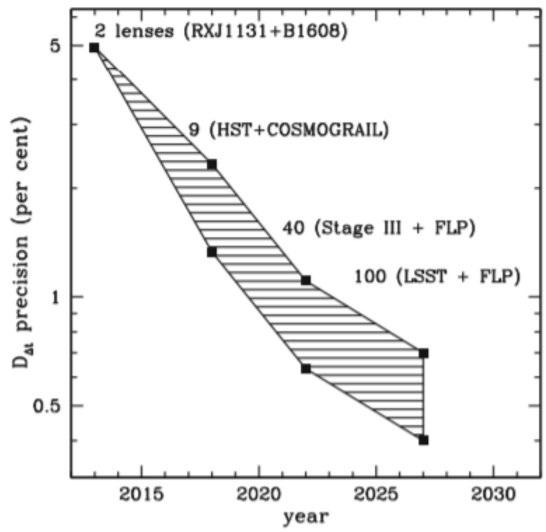

Figure 4: The improvement of the time delay distance measurement with future considerations ("FLP" indicates follow up observations paired with the surveys of note) [1].

4 Systematic Uncertainties Past and Future

Early time-delay analyses were frequently disputed due to problems in both measurement and analysis. The two primary controversies:

- At first, data quality allowed for non-unique solutions (multiple estimated values) due primarily to the effects of two phenomena on the analysis [11].
  - Gaps in the data
  - Optical light curves experiencing microlensing
- With improved monitoring, unrealistic assumptions in modeling the lens mass distribution led to highly varied results between groups [1]

With these problems remedied to certain degrees in the modern age, now strong lensing is done in three primary stages: time delay estimation from light curves, mass modelling of the lensing structure, and environment and line of sight modeling. The latter is especially important for amping up precision moving forward and is a relatively nascent addition to the technique.

Mass modelling is a systematic distinct to lensing as a cosmological probe, but lensing has the benefit of being independent of distance ladder calibrations like the Cepheid period-luminosity relation or using the tip of the red giant branch (TRGB). Problematic systematic uncertainties can arise from these standard candle measurements of distance as accurate flux measurements require properly accounting for dust, the interstellar medium (ISM), and airmass (when using ground-based observatories). Lensing, especially with time delays can avoid this entirely. Weak lensing, on the other hand, broadly depends on shape measurement and can be subject to systematics reliant on having a well understood point-spread-function (PSF) for the telescope optics. Some shared biases across most flux-limited surveys include Malmquist and Eddington bias in the samples examined, though this has little to do with the cosmological measurements in strong lensing and more to do with redshift assignment in weak lensing.

4.1 Observing Strategies and Constraints

Observing strategies rely on long-durations ("campaigns") of repeated visits to the system to best converge on Δt measurements and the resultant cosmological inferences. Desirable cadences are approximately on the order of 3 days. Accuracy, from past surveys and simulations seems to rely most on season length, while cadence appears to largely govern precision.

The Large Synoptic Survey Telescope (LSST) has a projected sampling gap of 4 to 5 days, longer than is ideal, over a season of about 4 months, which is the preferred season length. Given the survey limitations, it was projected that very few accurate measurements with time delays less than 10 days would be possible, restricting potential lenses to $10 < \Delta t < 120$ days [12]. This means that in spite of some mocked 2800 lenses being predicted to be seen for LSST, only a yield of 1900 lenses would first make the cut based on physical limitations and of those, only 20-30% had acceptably constrained Δts. An expected 400 or so lensed quasars should have measurable time delays out of this sample, and the study revealed this should be sufficient to do precision cosmology if catastrophic outliers are caught during the measurement process [12]. It is worthy of note that this study only used the mocked catalog from Oguri & Marshall 2010, while the paper suggests that LSST will see 8000 lensed quasars with 3000 well-measured time delays (an order of magnitude larger than available via the mocked catalog) [13].

Observing strategies moving forward will be governed by conflicting science goals. While LSST is designed to be synoptic and cover the entire footprint swiftly, other requirements set the observing cadence and season length along with this particular brand of time domain physics - namely the desire to catch interesting new time variability and supply real time alerts to other observatories. Effectively, limiting the cadence comes from an aim to cast a wide net and provide multimessenger data for previously unseen events. For the sake of strong lensing, this might be seen as a trade off between desire for a large number of lensed systems and the desire for higher sampling of those systems.

4.2 Microlensing

While one of the first high precision measurements of a strongly lensed system was made in the radio, optical telescopes are generally more accessible and eventually became the primary tool of choice for strong lensing studies.

There was a concern that optical light curves would have potentially higher systematic error due to microlensing events. Studies were done in preparation for the COSmological MOnitoring of GRAVItational Lenses (COSMOGRAIL) in 2005 that revealed this concern was somewhat unfounded. Simulations done in Eigenbrod et al. 2005 revealed that microlensing increased random error on Δt but did not significantly increase the systematic error [14]. As the aim for COSMOGRAIL was to make measurements of Δt with accuracies of 1-2%, microlensing did not appear to pose a real threat.

4.3 The Mass Distribution

Probing and understanding the mass distribution has historically been a difficult problem. If we only use time delay measurements, Eqn. 22 would indicate that uncertainty in the mass profile would lead to comparable uncertainty in Δt. If only the fixed image positions are given, there is a degeneracy in the *mass sheet transformation*, where no mass distribution would be significantly favored over another even in ideal lensing conditions, like perfect Einstein rings [15]. Since the distribution is described commonly as a power law, the slope of the profile is the primary parameter in question.

Independent measurements of the mass distribution are paramount then to get the best possible cosmological results from a lensing system. Some alternative avenues to examine the mass distribution include

1. Stellar kinematics of the lensing system,
2. Inferring luminosity of the lens system,
3. Inferring the absolute size of the lensing system,

with the first being the most generally applicable. As the stellar velocities and the time delays depend on the enclosed mass to different powers of the radius, the combination allows for an understanding of the scale of the lens galaxy. With this information, the angular separation *is* useful to probe the angular diameter distance [1].

In practice, other effects need to be taken into account to get a reliable model that agrees with all types of observations. A couple of these effects include additional weak lensing along the line of sight, and the need for incorporating external mass (filamentary structure and other galaxies that distort the images) into the model - usually seen as a constant convergence κ. If not constrained by other methods and merely allowed to be a nuisance parameter, H_0 has the potential to be strongly degenerate with this external convergence, further motivating proper modelling [8].

4.4 The Importance of Blinding

Given the breadth of available cosmological probes, it can be tempting for scientists to stop pursuing systematic error analysis when they have achieved some general community consensus. With the advent of potential Hubble constant tensions, which could be a product of systematics or unaccounted for physics, and even more precise measurements than ever before, rigorously handling systematic uncertainties *correctly* is paramount.

Blinding has therefore been introduced in other realms and has also been advocated for in time-delay distance measurements - notably implemented in the analysis for the RXJ1131–1231 system in Suyu et al. 2013 [16]. It will likely become common practice moving forward.

5 Constraining Ω_m and σ_8 with Weak Lensing

The matter fraction in the galaxy and the distribution tells us a great deal about large scale structure as well as the nature of dark matter. A parameter I have yet to introduce, σ_8 is of interest for the evolution of structure in the universe, as it describes the amplitude of the matter power spectrum at a scale of 8 Mpc/h. This was chosen traditionally as it was near to unity, though modern measurements put σ_8 at about 0.8. In a way, this encodes the formation of large scale structure and matter fluctuations within some generalized 8 Mpc region.

5.1 Using Late Era Galaxy Surveys

Since this is better explored in the domain of weak gravitational lensing, I will briefly outline the results and not the methodology. Weak lensing is a statistical effect that relies on the idea that the mean ellipticity of an ensemble of galaxies will be zero, unless in the presence of lensing structure. Correlation functions can then provide us with information on Ω_m.

Weak lensing requires high quality galaxy *shape* measurements. Converting the data from surveys to obtain weak lensing mass distributions requires:

- Masking bright stars that saturate the images and objects nearby to ignore the effects of gradient backgrounds.
- Masking asteroids and satellite trails as well as other select local astronomical sources.
- Identifying stars suitable for PSF modeling and having a suitable star - galaxy classification.
- Photometric redshifts to split the sample into tomographic bins.
- Reliable shape and shear measurement techniques, typically involving deconvolving the image with the PSF, applying an artificial shear, reconvolving, and measuring the change in shape.

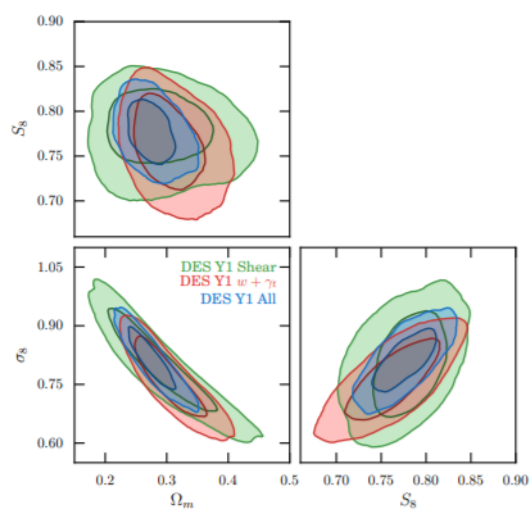

Figure 5: DESY1 weak lensing constraints on Ω_m and σ_8. Here S_8 is a rescaling of σ_8 with Ω_m to better view the distribution [17].

The estimation of redshifts (photo-zs) for galaxies is the major astrophysical uncertainty in weak lensing. Final sample selection cuts the measured galaxies according to the following properties, restricting to galaxies with well measured shapes [18]:

- Signal to Noise Ratio (SNR), as a measure of measured flux in a given band over the error in that measurement
- First order area moments, I_{xx}, I_{yy}, which more or less determine the centroid of the shape
- The total ellipticity, e

- The observed galaxy size, which depends on distance to the source and intrinsic size

The types of constraints in large surveys can be seen in Fig. 5 which reports on the $\Omega_m\sigma_8$ constraints provided by the Dark Energy Survey (DES) year 1 analysis [17]. With the later DES analyses and the deeper survey coming with LSST, the coarse matter distribution will be much better constrained. Broadly speaking, weak lensing in late era surveys puts constraints on the quantity $\Omega_m\sigma_8^{0.5}$ and can break degeneracy with tomographic bin slicing since the power of σ_8 constrained is related to mean redshift of the sample. Deeper surveys therefore allow for more tomographic bins, which help to disentangle Ω_m and σ_8 further. The cosmic shear constraint for DES is of a comparable statistical power to CMB lensing (discussed in the next section), but due to the lower mean redshift of the sources has a different degeneracy in the $\Omega_m - \sigma_8$ plane [19].

Synergy between the upcoming large surveys like LSST and Euclid have the potential to dramatically lower photometric redshift errors by incorporating high resolution Euclid fields into photo-z estimation [20]. Since most photo-z methods map colors into redshift space, spectroscopic samples and deep fields are crucial to making wide fields accurate and precise. Similar synergy is possible with other surveys catalog sharing and varying field selection, which will reduce overall systematic weak lensing errors.

5.2 Using CMB lensing for Degeneracy Breaking

Large scale structure between the last scattering surface and where we observe the cosmic microwave background (CMB) can contribute to measurable gravitational lensing effects within the CMB, both in apparent temperature variations as well as polarization. This is a surface-brightness conserving remapping of the CMB when emitted using the gradient of the projected potential. The lensing potential is well described by a Gaussian random field to first order as there are many lenses along a given line of sight and perturbations can be approximated fairly well with linear theory. Again, while the methodology will not be discussed thoroughly here, the implications on cosmological constraints will be.

If we average over the sky, lensing "smooths out" the initial power spectrum as well as the E-mode polarization peaks. While a relatively small effect, deep in the damping tail of the power spectrum the lensing can contribute up to an order of 10%, and has been detected via Planck. CMB power spectrum peaks fix the distance to recombination, and thus constrain $\Omega_m h^2$. Lensing observables in the CMB let us probe the structure and distance at high redshifts - cutting down on degeneracy between several parameters as seen in Fig. 5. Since lensing is a probe of structure and the matter distribution at high redshift, it constrains $\Omega_m\sigma_8^{0.25}$ where galaxy lensing constrains $\Omega_m\sigma_8^{0.5}$ when simply examining a single tomographic bin. This power variation has to do with redshift, as we examine the CMB as a relic of early times and galaxy surveys provide later information. We can how this can aid degeneracy breaking in parameter space using DES YR1 and Planck results together in Fig. 6 [21].

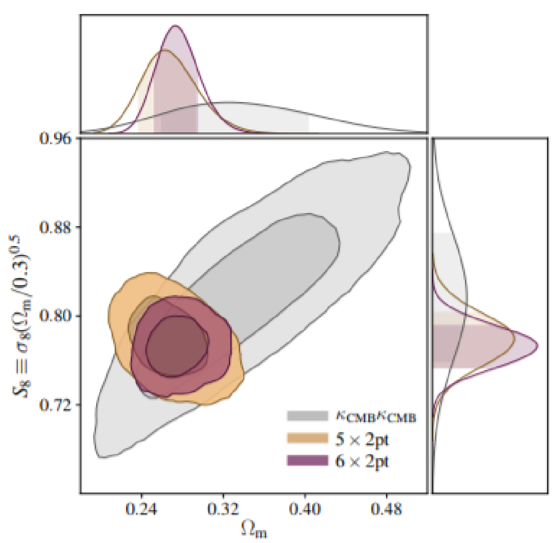

Figure 6: DES weak lensing constraints from varying correlation approaches paired with those given by CMB lensing in Planck, breaking degeneracy in Ω_m and S_8. Note how the two degeneracies are advantageously nearly orthonormal.

6 Conclusions

The coming decade will be an especially exciting era for cosmology, reaching an unprecedented synthesis of many independent measurement techniques to rigorously examine our understanding of the universe. Strong gravitational lensing is one of several promising fields that will soon provide measurements competitive with and eventually outpacing the current precision standard: the CMB.

We have shown that weak lensing and strong lensing studies complement one another by acting as probes for different cosmological parameters - H_0, Ω_Λ, and w being better constrained by strong lensing while Ω_m, and σ_8 are the primary measurements arising from weak lensing. It has also been demonstrated that each probe provides its own avenue for degeneracy breaking in this parameter space, the primary benefit of independent astrophysical probes.

The use of blinding, more sophisticated mass modelling, new observing strategies, and surveys that will discover over an order of magnitude more lenses as well as those that complete weak lensing studies will all contribute to yet another independent check on our measurements for ΛCDM and other cosmological models. Both strong and weak lensing will help probe the nature of dark energy, and though it was not discussed in this paper, strong lensing is and will be an excellent test to disentangle the nature of dark matter through halo and subhalo structure. We are at the cusp of learning much more about our universe and strong lensing is poised to become its most relevant, pushing into new territory that will undoubtedly reveal new and exciting science.

References

[1] Marshall P.J. Treu, T. Time delay cosmography. *Astronomy and Astrophysical Review*, (24), 2016.

[2] Y. Mellier. Cosmological applications of gravitational lensing, 1999.

[3] S.M. Carroll. *Spacetime and Geometry*. Cambridge University Press, 2019.

[4] P. Schneider. *Extragalactic Astronomy and Cosmology*. Springer-Verlag Berlin Heidelberg, 2015.

[5] Ehlers J. Falco E.E. Schneider, P. *Gravitational Lenses*. Springer-Verlag Berlin Heidelberg, 1992.

[6] Curtis McCully, Charles R. Keeton, Kenneth C. Wong, and Ann I. Zabludoff. A new hybrid framework to efficiently model lines of sight to gravitational lenses. *Monthly Notices of the Royal Astronomical Society*, 443(4):3631–3642, 08 2014.

[7] Danuta Paraficz and Jens Hjorth. THE HUBBLE CONSTANT INFERRED FROM 18 TIME-DELAY LENSES. *The Astrophysical Journal*, 712(2):1378–1384, mar 2010.

[8] Banafshe Shiralilou, Matteo Martinelli, Georgios Papadomanolakis, Simone Peirone, Fabrizio Renzi, and Alessandra Silvestri. Strong lensing time delay constraints on dark energy: a forecast, 2019.

[9] I. Jee, E. Komatsu, S.H. Suyu, and D. Huterer. Time-delay cosmography: increased leverage with angular diameter distances. *Journal of Cosmology and Astroparticle Physics*, 2016(04):031–031, apr 2016.

[10] Dan Coe and Leonidas A. Moustakas. COSMOLOGICAL CONSTRAINTS FROM GRAVITATIONAL LENS TIME DELAYS. *The Astrophysical Journal*, 706(1):45–59, oct 2009.

[11] William H. Press, George B. Rybicki, and Jacqueline N. Hewitt. The Time Delay of Gravitational Lens 0957+561. II. Analysis of Radio Data and Combined Optical-Radio Analysis. , 385:416, Feb 1992.

[12] Kai Liao, Tommaso Treu, Phil Marshall, Christopher D. Fassnacht, Nick Rumbaugh, Gregory Dobler, Amir Aghamousa, Vivien Bonvin, Frederic Courbin, Alireza Hojjati, and Neal Jackson et al. STRONG LENS TIME DELAY CHALLENGE. II. RESULTS OF TDC1. *The Astrophysical Journal*, 800(1):11, feb 2015.

[13] Masamune Oguri and Philip J. Marshall. Gravitationally lensed quasars and supernovae in future wide-field optical imaging surveys. *Monthly Notices of the Royal Astronomical Society*, page no–no, Apr 2010.

[14] Eigenbrod, A., Courbin, F., Vuissoz, C., Meylan, G., Saha, P., and Dye, S. Cosmograil: The cosmological monitoring of gravitational lenses - i. how to sample the light curves of gravitationally lensed quasars to measure accurate time delays. *A&A*, 436(1):25–35, 2005.

[15] Peter Schneider and Dominique Sluse. Mass-sheet degeneracy, power-law models and external convergence: Impact on the determination of the hubble constant from gravitational lensing. *Astronomy Astrophysics*, 559:A37, Nov 2013.

[16] S. H. Suyu, M. W. Auger, S. Hilbert, P. J. Marshall, M. Tewes, T. Treu, C. D. Fassnacht, L. V. E. Koopmans, D. Sluse, R. D. Blandford, F. Courbin, and G. Meylan. TWO ACCURATE TIME-DELAY DISTANCES FROM STRONG LENSING: IMPLICATIONS FOR COSMOLOGY. *The Astrophysical Journal*, 766(2):70, mar 2013.

[17] DES Collaboration. Dark energy survey year 1 results: Cosmological constraints from galaxy clustering and weak lensing. *Phys. Rev. D98*, (043526), 2018. https://arxiv.org/abs/1708.01530v3.

[18] Alexie Leauthaud, Richard Massey, Jean-Paul Kneib, Jason Rhodes, David E. Johnston, Peter Capak, Catherine Heymans, Richard S. Ellis, Anton M. Koekemoer, Oliver Le Fevre, and et al. Weak gravitational lensing with cosmos: Galaxy selection and shape measurements. *The Astrophysical Journal Supplement Series*, 172(1), 2007.

[19] Planck Collaboration. Planck 2018 results, vi cosmological parameters, 2018.

[20] Jason Rhodes, Robert C. Nichol, Éric Aubourg, Rachel Bean, Dominique Boutigny, Malcolm N. Bremer, Peter Capak, Vincenzo Cardone, Benoit Carry, Christopher J. Conselice, and et al. Scientific synergy between lsst andeuclid. *The Astrophysical Journal Supplement Series*, 233(2):21, Dec 2017.

[21] T.M.C. Abbott, F.B. Abdalla, A. Alarcon, S. Allam, J. Annis, S. Avila, K. Aylor, M. Banerji, N. Banik, E.J. Baxter, and et al. Dark energy survey year 1 results: Joint analysis of galaxy clustering, galaxy lensing, and cmb lensing two-point functions. *Physical Review D*, 100(2), Jul 2019.